EES Solar

MINIREVIEW

View Article Online
View Journal | View Issue

Cite this: *EES Sol.*, 2026, **2**, 108

Beyond organic photovoltaics: unlocking the potential of P3HT and its derivatives in perovskite and quantum dot solar cells

Kai Zhang, [a] Wenchao Zhao, *[b] Biao Xiao *[c] and Long Ye *[ac]

Poly(3-alkylthiophene)s (P3ATs), particularly poly(3-hexylthiophene) (P3HT), have emerged as promising materials for addressing interfacial challenges in perovskite and quantum dot solar cells. This mini review examines their evolution from simple hole transport layers to sophisticated interfacial engineering components through molecular design, multi-stack architectures, and composite strategies. We highlight how P3AT-based approaches mitigate limitations of conventional transport materials while enhancing device stability and performance. Recent progress in surface engineering, dopant-free processing, and blend-based optimization has driven notable performance improvements, yielding power conversion efficiencies above 25% in perovskite solar cells and 14% in quantum dot solar cells through the use of P3AT-based hole transport layers. The compatibility of P3ATs with scalable processing methods, combined with their tunable electronic properties and commercial availability, positions these materials as viable candidates for developing efficient, stable, and manufacturable next-generation photovoltaics. This critical analysis underscores the potential of P3AT-based strategies to overcome key challenges in emerging solar cell technologies.

Received 22nd September 2025
Accepted 2nd December 2025

DOI: 10.1039/d5el00154d

rsc.li/EESSolar

Broader context

The remarkable progress in perovskite and quantum dot solar cells has established them as leading contenders in next-generation photovoltaic technologies. However, their commercial viability faces significant challenges at critical interfaces, particularly in developing hole transport layers that combine high performance with long-term stability and scalable processing. Conventional small-molecule transport materials suffer from intrinsic limitations including dopant-induced degradation, batch-to-batch variability, high synthesis costs, and inadequate environmental stability. This mini review examines how poly(3-alkylthiophene)s (P3ATs), particularly P3HT, offer compelling solutions to these interfacial challenges through their unique combination of tunable energy levels, high intrinsic hole mobility, and robust film-forming properties. Their commercial availability, solution processability, and compatibility with large-scale manufacturing methods position them as ideal candidates for addressing the stability-cost-performance trade-offs that have hindered widespread adoption of emerging photovoltaic technologies. Looking forward, the strategic implementation of P3AT-based interfacial layers represents a crucial step toward developing photovoltaic devices that meet both performance benchmarks and practical requirements for commercial deployment, ultimately accelerating the transition to sustainable energy solutions.

1. Introduction: benchmark materials in emerging photovoltaics

Photovoltaic devices, commonly referred to as solar cells, are electronic devices that harness renewable energy from the sun and convert sunlight directly into electricity. Solar cells, as an increasingly attractive and viable option for renewable energy generation, offer numerous advantages for meeting global energy needs while reducing carbon emissions. They can reduce reliance on fossil fuels, mitigate greenhouse gas emissions, and contribute to the transition to a more sustainable and low-carbon energy system. Poly(3-alkylthiophene)s (P3ATs), with poly(3-hexylthiophene) (P3HT) as the most prominent representative,[1,2] have participated more actively in the history of organic photovoltaics[3–8] (OPVs). Their regioregular backbone, favorable π–π stacking, and straightforward solution processing enabled early advances in bulk heterojunction solar cells and helped define the framework of polymer-based photovoltaic research.[9–13] Nonetheless, with the advent of high-performance donor–acceptor polymers and non-fullerene acceptors, P3ATs have gradually been displaced from the forefront of OPV efficiency records.

[a]*School of Materials Science and Engineering, Tianjin Key Laboratory of Molecular Optoelectronic Sciences, Key Laboratory of Organic Integrated Circuits, Ministry of Education, Collaborative Innovation Center of Chemical Science and Engineering, State Key Laboratory of Advanced Materials for Intelligent Sensing, Tianjin University, Tianjin 300072, China. E-mail: yelong@tju.edu.cn*

[b]*Co-Innovation Center of Efficient Processing and Utilization of Forest Resources, College of Materials Science and Engineering, Nanjing Forestry University, Nanjing 210037, China*

[c]*Key Laboratory of Optoelectronic Chemical Materials and Devices of Ministry of Education, Jianghan University, Wuhan, China*

Despite this transition, renewed interest in P3ATs has emerged in the context of perovskite solar cells (PSCs)[14,15] and quantum dot solar cells (QDSCs).[16–19] In these devices, where interfacial phenomena critically determine charge transport, recombination, and long-term stability, P3ATs have been increasingly recognized not as primary light absorbers but as interfacial mediators. In QDSCs, conventional hole transport layers (HTLs) often rely on solid-state ligand exchange and layer-by-layer processing methods.[20] These approaches are not only technologically cumbersome but also introduce significant limitations for large-scale manufacturing and commercial viability. In contrast, organic semiconductors offer distinct processing advantages,[21] including compatibility with solution-based deposition techniques and scalability, attributes that position them as promising candidates for simplifying QDSCs device fabrication. Similarly, in PSCs, while typical hole transport materials such as spiro-OMeTAD,[22] poly(triaryl amine) (PTAA)[23] and self-assembled monolayers (SAMs)[24] have enabled remarkable device efficiencies, they face inherent limitations. Spiro-OMeTAD requires chemical doping to achieve sufficient conductivity and appropriate energy level alignment, but these dopants often compromise morphological and thermal stability,[25] leading to device degradation under operational conditions. PTAA, though exhibiting good interfacial properties, suffers from high synthesis cost, batch-to-batch variability, and similarly relies on hygroscopic dopants. SAM-based HTLs also suffer from intrinsic photochemical instability and unreliable anchoring to ITO, which together lead to accelerated interfacial degradation under device operation (Table 1).

Within this context, P3ATs have regained attention as promising HTL materials owing to a combination of favorable electronic, morphological, and processing attributes.[33] Their tunable energy levels facilitate efficient hole extraction from both perovskite and quantum layers while providing adequate electron blocking. Perhaps more importantly, P3ATs exhibit relatively high intrinsic hole mobility in the solid state, reducing or eliminating the need for exogenous dopants. This dopant-free operation mitigates degradation pathways associated with mobile ions and morphological instability, thereby enhancing device longevity. Furthermore, the semi-crystalline nature of P3HT[34] promotes the formation of robust, uniform films, while its hydrophobic side chains contribute to moisture resistance. From a practical standpoint, P3HT is produced commercially at low cost with high batch-to-batch consistency,[28] and it is readily processed using scalable methods such as blade coating and inkjet printing. These characteristics make P3ATs particularly attractive as HTLs in both PSCs and QDSCs, where they can simultaneously address performance, stability, and manufacturability constraints (Fig. 1). In this mini review, the state-of-the-art use of P3ATs in PSCs and QDSCs is critically examined. The focus is placed on their functions as HTLs, both as direct applications and within multi-layer configurations, their integration into composite transport structures *via* blending or doping, and their exploratory use in hybrid absorbers. Through this analysis, the evolving role of P3ATs is considered in relation to interfacial engineering and device stability in emerging photovoltaic systems. We anticipate that this overview will serve as a foundation for advancing interfacial engineering strategies and improving the operational stability of emerging photovoltaic systems and diverse devices.

Kai Zhang

Kai Zhang received his BS degree in Materials Science and Engineering from Tianjin University in 2023. He is now a PhD candidate at the School of Materials Science and Engineering, Tianjin University, under the supervision of Prof. Long Ye. His research interest mainly focuses on the characterization and analysis of polymer condensed structures and fabrication of high-performance optoelectronic devices.

Long Ye

*Long Ye has been a professor at the School of Materials Science and Engineering, Tianjin University since October 2019. He received his PhD degree from the Institute of Chemistry, Chinese Academy of Sciences in 2015 (Advisor: Prof. Jianhui Hou). From 2015 to 2019, he was a postdoctoral researcher (Advisor: Prof. Harald Ade) and later promoted to research assistant professor at the Department of Physics, North Carolina State University. His current interests include flexible/stretchable organic optoelectronic devices and related materials physics (*e.g.*, aggregate structure, thermodynamics, mechanics).*

2. Direct application and interfacial engineering

The initial investigation of P3ATs as HTLs in PSCs and QDSCs was motivated by their commercial availability, solution processability, and lower cost compared to other small-molecule alternatives.[35] The performance of pristine P3ATs as HTLs is influenced by their molecular characteristics and the resulting film morphology. Key parameters such as molecular weight, regioregularity, and side-chain architecture govern the degree of crystallinity and molecular packing, thereby critically influencing the hole mobility. For instance, Carlo *et al.*[36,37] reported that P3HT with higher molecular weight and lower regioregularity preferentially adopted a face-on stacking orientation and formed flatter HTLs, leading to improved power conversion efficiency (PCE) in PSCs. Beyond the widely studied P3HT,

Table 1 Comparison of key metrics for representative hole-transport layer (HTL) materials in perovskite and quantum dot solar cells

HTL materials	Power conversion efficiency (PCE)	Stability	Cost	Processing complexity	Mechanical flexibility	Ref.
P3ATs	25.16% (PSCs)	MPP-T_{96}[a] ~ 2030 h	Low (<\$10 g^{-1})	Simple (solution processable; dopant-free possible)	High	26–28
	14.28% (PbS QDSCs)	MPP-T_{90} ~ 520 h				
Quantum dots	12.60% (PbS QDSCs)	MPP-T_{90} ~ 3 h	Low-moderate	Moderate (ligand exchange; multi-step processing)	Low	29
Spiro-OMeTAD	25.45% (PSCs)	MPP-T_{90} ~ 1000 h	Very high (>\$300 g^{-1})	Complex (requires doping; sensitive to O_2/H_2O)	Low	30
PTAA	26.17% (PSCs)	MPP-T_{90} ~ 140 h	High (>\$200 g^{-1})	Simple (solution processable; dopant-free possible)	Moderate	31
SAMs	27.20% (PSCs)	MPP-T_{86} ~ 1530 h	Moderate	High (controlled surface chemistry; ultrathin films difficult to optimize)	Very low	32

[a] MPP refers to the maximum power point under AM 1.5 illumination. T_x denotes the time required for the device's PCE to decay to x% of its initial value (*e.g.*, T_{96} = time to reach 96% of initial PCE).

structurally simple derivatives have also been investigated. Liu *et al.*[9] reported that poly(3-pentylthiophene) (P3PT) exhibits reduced molecular aggregation and a preferential face-on orientation, properties that are favorable for hole transport. Building on this observation, Wu *et al.*[38] employed P3PT as a direct replacement for P3HT in $FA_{0.84}MA_{0.16}PbI_3$ PSCs and PbS QDSCs, resulting in PCE enhancements from 16.0% to 18.8% and from 8.6% to 9.5%, respectively (Fig. 2a and b). These results highlight the potential of alternative P3AT derivatives as simple yet effective HTL candidates.

Despite these advances, the direct use of pristine P3ATs as HTLs remains limited by intrinsic drawbacks. One critical issue is the frequent misalignment between the highest occupied molecular orbital (HOMO) level of P3ATs and the valence band of common perovskites and quantum dots, which introduces an energy barrier that hinders efficient hole extraction and lowers the open-circuit voltage. In addition, their semi-crystalline and hydrophobic nature often leads to poor surface coverage, pinholes, and suboptimal interfacial contact, resulting in increased non-radiative recombination. These electronic and morphological limitations ultimately constrain both device efficiency and reproducibility. To address these challenges, research has increasingly focused on perovskite surface engineering to reduce defects and improve interfacial contact. Effective strategies have been developed to tailor perovskite interfacial properties. Sun *et al.*[39] addressed surface defects in δ phase $CsPbI_2Br$ film by introducing potassium trifluoroacetate, facilitating secondary crystal growth during the δ → α phase transition (Fig. 2c). The subsequent incorporation of a P3HT hole transport layer yielded a device efficiency of 17.1%. Li *et al.*[40] developed a hydrogen-bond-assisted dimethylammonium (DMA) extraction strategy to fabricate γ-$CsPbI_3$ films. Hydrogen bonding between polyacrylic acid and $DMAPbI_3$ lowered the DMA escape barrier, accelerating

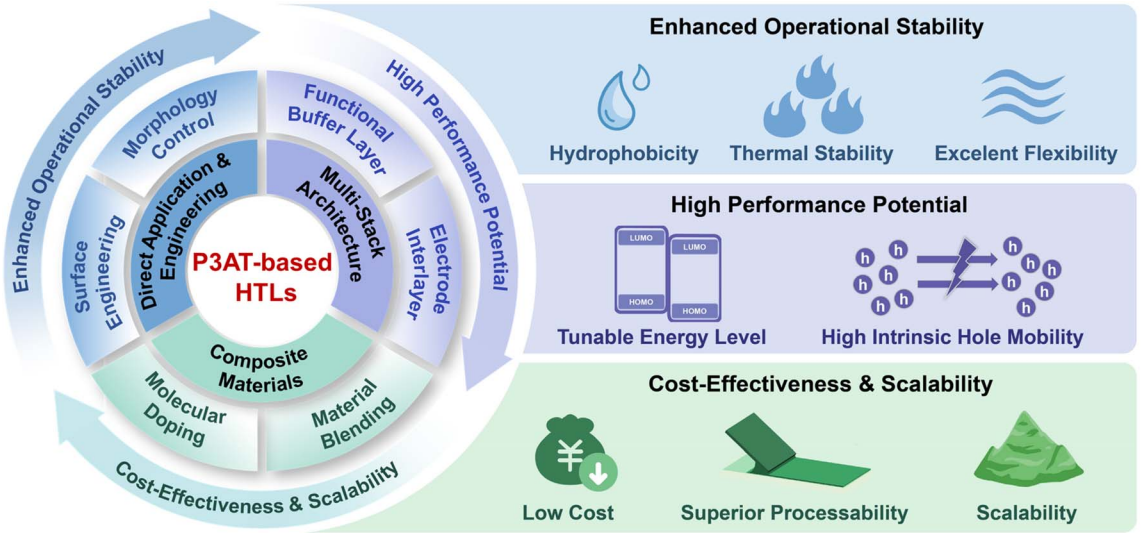

Fig. 1 Application strategies of P3AT-based hole transport layers (HTLs) in perovskite and quantum dot solar cells, highlighting their multi-functional advantages in operational stability, performance potential, and cost-effective scalability.

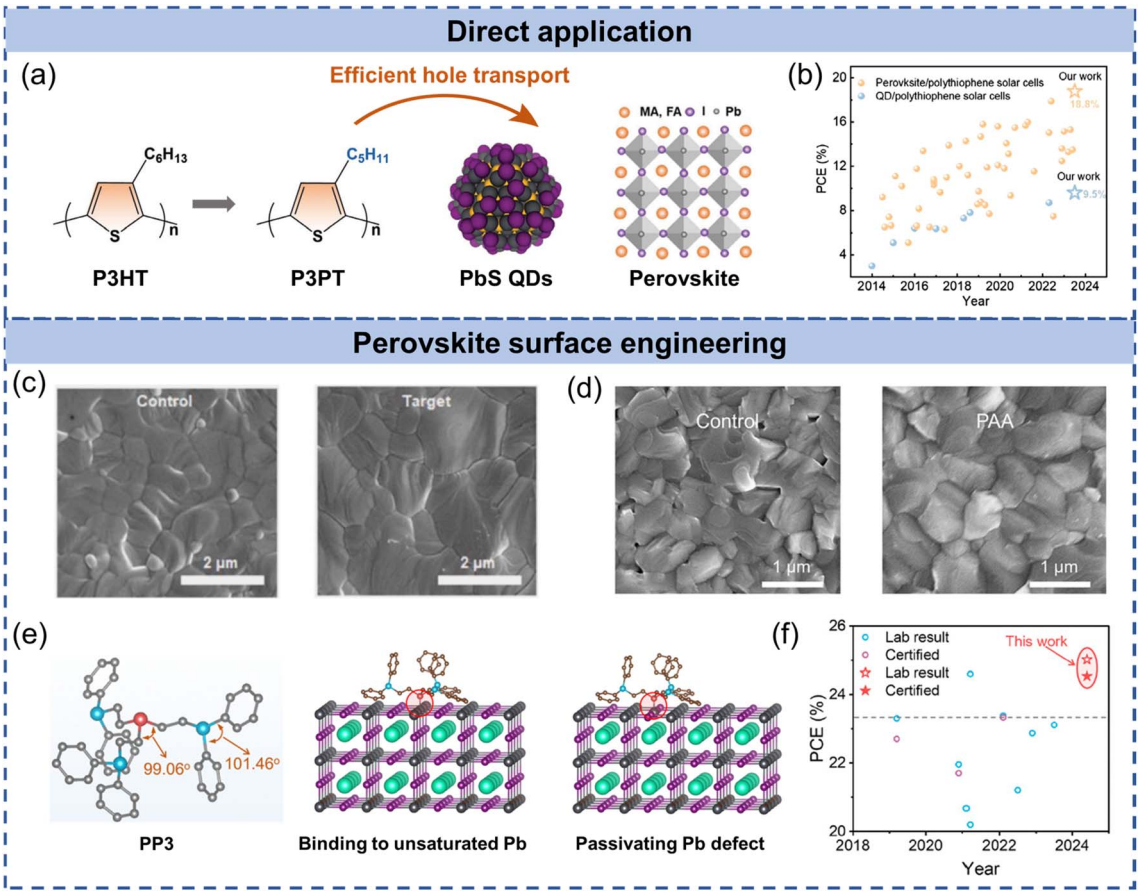

Fig. 2 (a) The schematic of efficient hole transport from PbS QDs or perovskite active materials to P3PT HTMs. The difference between P3HT and P3PT is denoted. Reproduced with permission.[38] Copyright 2024, Wiley. (b) The progress of perovskite/polythiophene solar cells and QD/polythiophene solar cells and our contribution. Reproduced with permission.[38] Copyright 2024, Wiley. (c) SEM images of $CsPbI_2Br$ films before and after interface engineering. Reproduced with permission.[39] Copyright 2023, Elsevier. (d) Top-view SEM images of control and PAA processed films. Reproduced with permission.[40] Copyright 2023, Elsevier. (e) Spatial configuration of phosphine ligands and structural optimization of PP3 for binding to unsaturated Pb and passivating PbI antisite defects. Reproduced with permission.[41] Copyright 2024, The Royal Society of Chemistry. (f) Efficiency evolution of state-of-the-art $CsFAPbI_3$ PSCs with dopant-free P3HT HTLs. Reproduced with permission.[41] Copyright 2024, The Royal Society of Chemistry.

$DMAPbI_3$ decomposition and $CsPbI_3$ crystallization. This process yielded pinhole-free $CsPbI_3$ films free of $DMAPbI_3$ residues (Fig. 2d), enabling dopant-free P3HT-based solar cells with 20.25% PCE and well moisture and operational stability. Similarly, Jeong *et al.*[42] and Ren *et al.*[43] enhanced interfacial contact with P3HT HTL by introducing sodium formate and ethyl cyanoformate, respectively, to regulate perovskite crystallization and passivate interfacial defects. More recently, Li *et al.*[41] developed a versatile molecular engineering strategy employing tailorable phosphine ligands to optimize the perovskite/P3HT interface, effectively reducing recombination losses and maximizing device voltage. This approach enabled $CsFAPbI_3$ perovskite solar cells to achieve top-tier efficiencies of 25.08% (Fig. 2e).

3. Multi-stack transport architectures

Beyond interfacial modification, the incorporation of multi-stack transport layers has emerged as a powerful strategy to further improve device performance. This approach can be employed to optimize energy-level alignment at the active layer/HTL and HTL/electrode interfaces or to strengthen interfacial contact. In this context, carefully engineered multifunctional small molecules have frequently been employed as buffer layers. In 2019, Jung *et al.*[14] introduced a double-layered halide architecture (Fig. 3a), in which a wide-bandgap ionic molecule, *n*-hexyl trimethyl ammonium bromide, interlayer was inserted between the perovskite and P3HT. Rather than simply modifying interfacial interactions, the wide-bandgap halide layer increased the flat-band potential of the device and promoted the self-assembly of P3HT at the perovskite surface. This strategy enhanced van der Waals interactions at the interface and suppressed non-radiative recombination, resulting in a record PCE of 23.3%. Building on this concept, Wang *et al.*[44] and Choi *et al.*[45] employed other ionic molecules as buffer layers to mitigate surface defects in perovskite, thereby improving interfacial contact with P3HT. Song *et al.*[46] designed and synthesized the small molecule BTCIC-4Cl as an intermediate

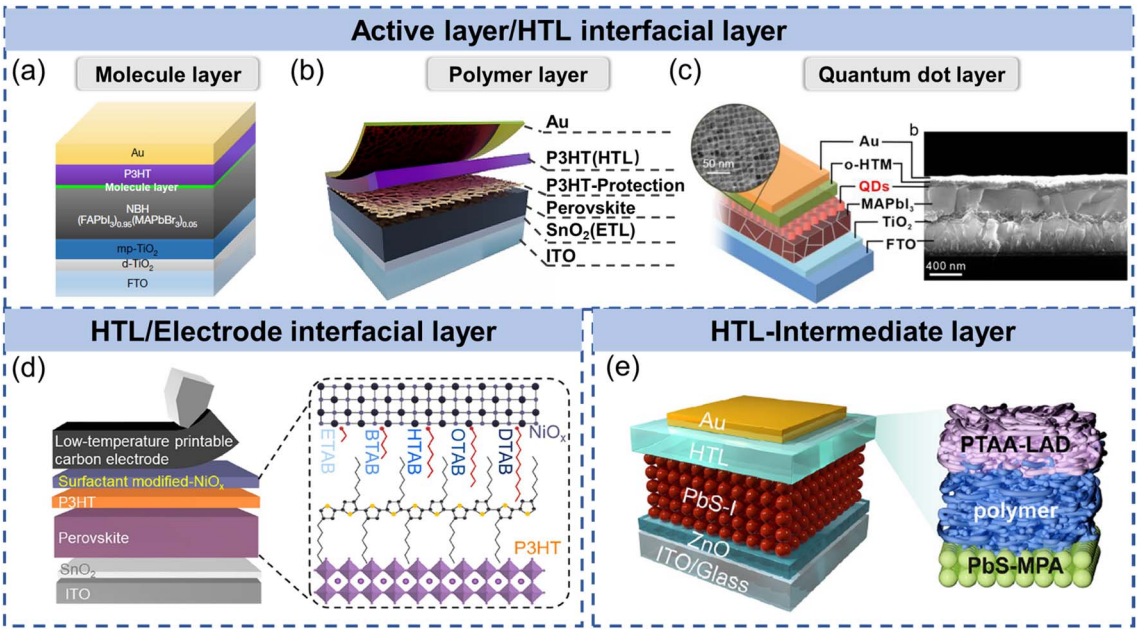

Fig. 3 (a) The structure of an n-i-p perovskite solar cell based on wide-bandgap ionic molecule using P3HT as the hole-transport material. Reproduced with permission.[14] Copyright 2019, Springer Nature. (b) The structure of perovskite device with P3HT-protection layer. Reproduced with permission.[49] Copyright 2024, The Royal Society of Chemistry. (c) Schematic of PSC structure and representative TEM image of $CsPbI_{1.85}Br_{1.15}$ QDs. Reproduced with permission.[50] Copyright 2021, American Chemical Society. (d) Schematic illustration of low temperature printable C-PSC using P3HT/NiO_x bilayer HTLs modified with different chain-length surfactants. Reproduced with permission.[51] Copyright 2025, American Chemical Society. (e) Device structure of the solar cell and schematic diagram of multi-stack transport layers. Reproduced with permission.[27] Copyright 2025, Wiley.

layer, enabling $CsPbI_2Br$/BTCIC-4Cl/P3HT PSCs to reach 16.3% efficiency with negligible PCE loss after 500 hours of thermal annealing. Similarly, Gu *et al.*[47] and Li *et al.*[48] synthesized molecular acids that effectively passivated undercoordinated Pb^{2+} defects and improved interfacial contact between P3HT and perovskite.

Polymeric and nanostructured interlayers have also been widely investigated. Li *et al.*[52] enhanced the energy-level alignment between $CsPbI_2Br$ and P3HT by introducing a diphenylamine-derived polymer buffer layer, whose deeper HOMO (−5.30 eV) creates a graded cascade between the perovskite (HOMO −6.08 eV) and P3HT (HOMO −5.14 eV), thereby facilitating hole extraction and enabling an open-circuit voltage of 1.26 V (Fig. 3b). Likewise, Zhang *et al.*[53] employed a polyelectrolyte buffer layer with a HOMO of −5.22 eV, which suppressed interfacial recombination and yielded a PCE of 19.2%. Recently, Roy *et al.*[49] proposed a polymeric protection layer strategy, in which $CsPbI_2Br$ was treated with P3HT during crystallization to form a protective interfacial layer (Fig. 3c), followed by the deposition of P3HT as the hole-transport layer. This approach effectively suppressed surface recombination and markedly improved the device's resistance to moisture and oxygen. Complementarily, Cheng *et al.*[50] introduced perovskite quantum dots (QDs) as a multifunctional interlayer between $MAPbI_3$ and P3HT. Ultraviolet photoelectron spectroscopy measurements showed that the QDs exhibit a HOMO level (−5.30 eV) that lies between that of $MAPbI_3$ (−5.40 eV) and P3HT (−5.20 eV after QD treatment; pristine P3HT −5.04 eV), thereby establishing a well-defined graded cascade that promotes more efficient hole extraction. In addition to improving energetic alignment, the QD layer also passivated interfacial defects and reduced charge-transfer resistance, collectively boosting the PCE of $MAPbI_3$-based devices from 16% to 21%.

The multi-stack approach has also been extended to improve interfacial contact with electrodes. Tan *et al.*[54] introduced nickel oxide (NiO_x) as an interlayer to optimize energy-level alignment across the perovskite/HTL/electrode stack. The graded alignment from perovskite (−5.91 eV) to P3HT (−5.30 eV) to NiO_x (−4.92 eV), along with the favorable contact with carbon (−4.82 eV), lowers interfacial barriers and enhances hole transfer and charge collection. They later incorporated brominated quaternary ammonium surfactants[51] into NiO_x nanoparticles to further facilitate hole transport (Fig. 3d), enabling printable carbon-based PSCs to achieve a PCE of 22.1%. Recently, Wen *et al.*[27] proposed a dual-interface engineering strategy to optimize surface energy matching and energy-level alignment. By introducing a thiol-exchanged ultrathin PbS quantum dot layer beneath P3HT and a doped PTAA layer above (Fig. 3e), they achieved improved interfacial contact and energy transfer across both interfaces. This configuration optimized both surface energy and energy-level alignment, resulting in PbS-based QDSCs with a record efficiency of 14.28%. Unencapsulated devices retained 90% of their initial efficiency after 520 hours under ambient conditions, highlighting the excellent stability achievable through such multi-interface engineering.

4. Composite transport layers *via* doping and blending

Building on the progress achieved through interfacial modification and multi-stack transport layers, further optimization of P3ATs as HTLs has focused on tuning its intrinsic electronic and morphological properties. A particularly effective strategy is molecular doping, which enhances charge carrier density and conductivity, thereby improving hole extraction efficiency. Traditional p-type dopants such as 2,3,5,6-tetrafluoro-7,7,8,8-tetracyanoquinodimethane (F4-TCNQ) have been widely employed to increase P3HT conductivity[55] by facilitating charge transfer from the polymer backbone. While such approaches significantly improve hole mobility, their impact on long-term stability and interfacial compatibility remains limited, constraining device reproducibility.

To overcome the limitations of traditional dopants, recent strategies have focused on simultaneously enhancing conductivity and regulating interfacial interactions. For instance, Jeong *et al.*[56] incorporated gallium(III) acetylacetonate directly into P3HT, enabling spontaneous interfacial engineering and yielding a PSC with a PCE of 24.6%. Li *et al.*[57] further advanced this strategy by doping P3HT with the conjugated small molecule SMe-TATPyr, which uniformly intercalates within the polymer matrix and disrupts the long-range in-plane ordering of P3HT. Grazing incidence wide-angle X-ray scattering (GIWAXS) analysis reveals that this disruption breaks large edge-on domains and induces the formation of face-on π–π-stacked clusters (Fig. 4a and b), thereby enabling more efficient vertical charge transport. This molecular-level reorientation increases hole mobility by nearly fourfold while simultaneously lowering surface defect density by more than 50%. Likewise, Lv *et al.*[58] synthesized doped organic salts that enhanced P3HT crystallization and reduced surface defects in the perovskite layer. Xu *et al.*[59] pursued a molecular bridge strategy, in which malononitrile groups anchored to the perovskite surface while triphenylamine moieties π–π stacked with P3HT, forming a continuous charge-transport channel that suppressed interfacial defects and nearly doubled device efficiency (Fig. 4c and d). More recently, Liu *et al.*[26] employed Spiro-TFSI as a radical-cation dopant for P3HT, where GIWAXS analysis showed that the dopant suppresses the native edge-on orientation by increasing the out-of-plane (010) π–π stacking intensity, indicating a shift toward face-on packing. *In situ* absorption measurements further revealed that Spiro-TFSI triggers rapid pre-nucleation of crystalline P3HT in solution (Fig. 4e and f), leading to a reorganized crystallization process during film formation. This dopant-induced structural reorientation, together with strong charge-transfer interactions, enhances vertical charge transport and enables PSCs to reach a record 25.16% efficiency with excellent stability.

Beyond molecular doping, another promising strategy to optimize P3ATs as HTLs is blending with complementary materials to overcome its intrinsic limitations. While doping primarily regulates charge density and stacking orientation, blending offers additional pathways to tune energy levels, enhance interfacial contact, and improve film morphology. Inorganic[61,62] and metal-based compounds, including oxides and phthalocyanines, have been widely employed as blending partners due to their intrinsic stability and favorable energy-level alignment. For instance, Liu *et al.*[63] incorporated zinc phthalocyanine into P3HT as a HTL, enabling $CsPbBr_3$ carbon-based PSCs to achieve a PCE of 10%. Likewise, Peng *et al.*[64] achieved a 23% PCE by blending P3HT with copper phthalocyanine and coupling it with a patterned TiO_2 electron transport layer. Cao *et al.*[60] blended NiO_x with P3HT as a HTL, where P3HT enhanced NiO_x film uniformity while NiO_x induced favorable orientation in P3HT, together improving hydrothermal stability and boosting PCE from 16% to 21% (Fig. 4g and h). More recently, Kim *et al.*[65] blended nickel phthalocyanine with P3HT, and by tuning their ratio during spin-coating, induced controlled phase separation that yielded a bilayer HTL with nickel phthalocyanine at the bottom and P3HT on top. This self-organized bilayer facilitated efficient hole transport, yielding a PCE of 23%.

While inorganic and metal-based additives can enhance interfacial contact and energy-level alignment, achieving more precise morphological regulation often requires structurally compatible partners. Consequently, blending P3ATs with organic semiconductors has also proven effective in modulating its morphology and charge transport. In 2022, an initial attempt[19] was made by blending a brominated version (P3HT-Br) of P3HT with P3HT itself. Blending P3HT with P3HT-Br induced a stronger face-on orientation (Fig. 5a), thereby facilitating more efficient charge transport. This approach increased the PCE of PbS quantum dot solar cells by 26% (Fig. 5b) and significantly improved thermal stability, with devices retaining 80% of their initial efficiency after 400 h at 85 °C. Qi *et al.*[66] further validated this effect by blending P3PT with P3HT, which optimized the organic film microstructure, raising PCE from 8.67% to 10.51%—among the highest reported for polythiophene/quantum dot solar cells. More recently, this strategy has been extended to PSCs. Yao *et al.*[67] blended P3HT with the conjugated polymer PM6, finding that the two polymers spontaneously intertwined into micrometer-scale fiber crystals (Fig. 5c) that provided efficient charge-transport pathways, accelerating hole extraction and boosting PCE from 22.9% to 24.9% (Fig. 5d). PTAA has also been widely adopted as a blending partner. Li *et al.*[68] showed that coordination between sulfur atoms in P3HT and Pb^{2+} ions reduced interfacial defect density and suppressed non-radiative recombination, while Tong *et al.*[69] revealed that PTAA promotes the face-on orientation of P3HT (Fig. 5e and f), and the simultaneous alignment of both polymers enhances interfacial passivation, thereby enabling more efficient charge transport.

In addition to the blending strategies discussed above, other explorations include blending P3HT with quantum dots[70] and with Spiro-OMeTAD,[71] further diversifying its applications as an HTL. Overall, blending enables synergistic regulation of morphology, energy levels, and interfacial interactions, complementing the effects of molecular doping. These strategies not only enhance conductivity and charge transport but also improve film stability and interface passivation, highlighting

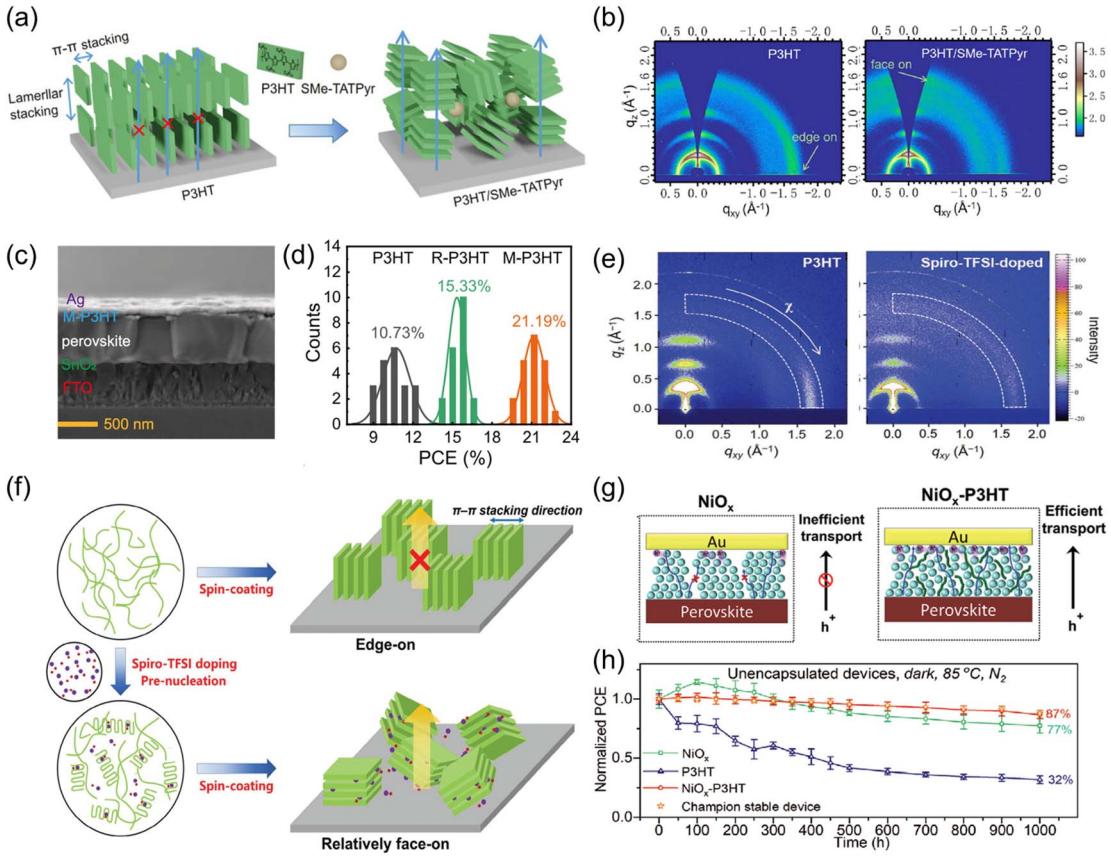

Fig. 4 (a) Schematic diagram of the molecular stacking. Reproduced with permission.[57] Copyright 2024, Wiley. (b) 2D GIWAXS patterns of undoped P3HT and SMe-TATPyr-doped P3HT. Reproduced with permission.[57] Copyright 2024, Wiley. (c) Cross-sectional SEM image of PSC with doped P3HT. Reproduced with permission.[59] Copyright 2022, Springer Nature. (d) PCE of PSCs without and with the molecular-bridge strategy. Reproduced with permission.[59] Copyright 2022, Springer Nature. (e) 2D GIWAXS patterns of undoped P3HT and Spiro-TFSI-doped P3HT. Reproduced with permission.[26] Copyright 2024, Wiley. (f) Illustration of Spiro-TFSI regulating the crystallization process of P3HT. Reproduced with permission.[26] Copyright 2024, Wiley. (g) Schematic illustration of PSC device structure and the engineering effect of NiO_x-based HTLs. Reproduced with permission.[60] Copyright 2022, Wiley. (h) Hydrothermal stability performance of unencapsulated PSCs. Reproduced with permission.[60] Copyright 2022, Wiley.

the potential of composite HTLs for achieving high-performance and durable solar cells.

5. Summary and outlook

The recent investigation of P3ATs in perovskite and quantum dot solar cells builds naturally on their well-established role in organic photovoltaics over the last two decades, taking advantage of their well-characterized electronic structure, processability, and semi-crystalline morphology. As summarized in this mini review, substantial progress has already been made in new emerging solar technologies: P3ATs have evolved from simple dopant-free HTLs to components integrated within engineered interfaces, multi-stack transport architectures, and composite layers designed to enhance energy-level alignment, suppress interfacial recombination, and improve charge extraction efficiency. These advances have contributed to measurable gains in PCE, stability, and manufacturability in both PSCs and QDSCs.

Despite these achievements, several unresolved challenges remain and represent opportunities for future work. One outstanding issue concerns the structure-mechanics trade-off in P3ATs: while high crystallinity enhances vertical charge mobility, it often reduces ductility, complicating the realization of flexible or stretchable photovoltaic modules. Strategies that decouple crystallinity from brittleness, through molecular-weight control, side-chain engineering, or block-copolymer design, are therefore key targets for future development. Another important knowledge gap involves the long-term evolution of interfacial defects at P3AT/perovskite and P3AT/quantum dot interfaces. Under sustained illumination and thermal stress, defect generation and ion migration can accelerate performance loss, yet the mechanisms remain insufficiently resolved. Understanding these processes will require *operando* characterization tools capable of probing buried interfaces, such as *in situ* GIWAXS, ambient-pressure photoelectron spectroscopy, and bias- or light-dependent scanning probe techniques.

In addition, several areas represent issues already partly addressed but needing further refinement. For example, multi-stack interlayers and molecular bridge strategies have shown

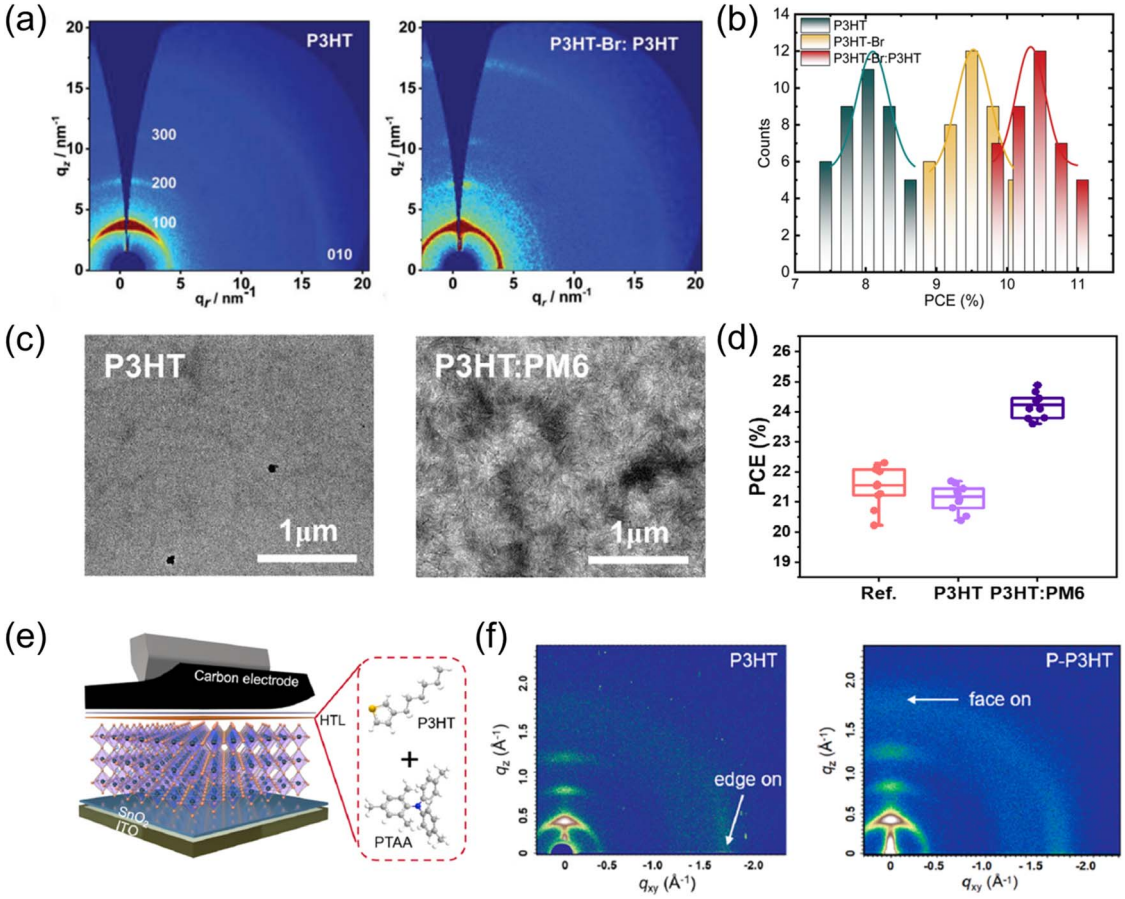

Fig. 5 (a) 2D GIWAXS patterns of P3HT and its blend with P3HT-Br. Reproduced with permission.[19] Copyright 2022, Wiley. (b) PCE histograms of QD/polythiophene hybrid solar cells. Reproduced with permission.[19] Copyright 2022, Wiley. (c) Transmission electron microscopy images of P3HT and P3HT:PM6 films. Reproduced with permission.[67] Copyright 2025, Wiley. (d) Statistical parameters based on PCE values of PSCs prepared from different HTLs materials. Reproduced with permission.[67] Copyright 2025, Wiley. (e) Schematic diagram of a low-temperature printable C-PSC and chemical structure of P3HT and PTAA. Reproduced with permission.[69] Copyright 2024, Elsevier. (f) GIWAXS patterns of P3HT and PTAA-P3HT HTLs. Reproduced with permission.[69] Copyright 2024, Elsevier.

promise in improving band alignment and chemical passivation, but broader design rules that connect molecular structure to interfacial energetics are still emerging. Similarly, recent progress in blade-coating, inkjet printing, and slot-die coating demonstrates that P3AT-based HTLs can be compatible with scalable manufacturing; however, maintaining nanoscale morphological control under high-throughput conditions remains a practical constraint. Finally, the transition toward commercialization will depend on a deeper integration of materials design, interfacial engineering, and scalable processing. For P3AT-based composite layers, understanding and convincingly analyzing the solution aggregation structures with advanced X-ray/neutron scattering and liquid-phase imaging are vital to their device function. Future research should prioritize models and characterization tools that unify these aspects, bridging fundamental structure–property relationships with manufacturing-relevant performance metrics such as operational stability, defect tolerance, and mechanical robustness.[72–78]

Overall, P3AT-based HTLs remain compelling candidates for next-generation photovoltaic technologies due to their tunable optoelectronic properties,[79] dopant-free functionality, and excellent cost-scalability balance. Continued research that addresses the remaining scientific and engineering challenges will further unlock the potential of this versatile polymer class in delivering efficient, stable, and manufacturable perovskite and quantum dot solar cells. Looking ahead, the current research of P3AT can be further expanded to other classes of conjugated polymers[80,81] and diverse functional devices.[82,83]

Conflicts of interest

The authors declare no competing financial interest.

Data availability

No primary research results, software or code have been included and no new data were generated or analyzed as part of this review.

Acknowledgements

The authors are grateful for the financial support from the Science Fund for Distinguished Young Scholars of Tianjin Municipality (No. 23JCJQJC00240), the opening project of Key Laboratory of Optoelectronic Chemical Materials and Devices of Ministry of Education, Jianghan University (No. JDGD-202304), the start-up grant of Peiyang scholar program from Tianjin University, and the fundamental research funds for the central universities.

References

1 J. Peng and Y. Han, *Giant*, 2020, **4**, 100039.
2 A. T. Kleinschmidt, S. E. Root and D. J. Lipomi, *J. Mater. Chem. A*, 2017, **5**, 11396–11400.
3 L. Li, F. Zhang, J. Wang, Q. An, Q. Sun, W. Wang, J. Zhang and F. Teng, *Sci. Rep.*, 2015, **5**, 9181.
4 Y. Kim, S. Cook, S. M. Tuladhar, S. A. Choulis, J. Nelson, J. R. Durrant, D. D. C. Bradley, M. Giles, I. McCulloch, C.-S. Ha and M. Ree, *Nat. Mater.*, 2006, **5**, 197–203.
5 S. Holliday, R. S. Ashraf, C. B. Nielsen, M. Kirkus, J. A. Rohr, C. H. Tan, E. Collado-Fregoso, A. C. Knall, J. R. Durrant, J. Nelson and I. McCulloch, *J. Am. Chem. Soc.*, 2015, **137**, 898–904.
6 T. Bura, J. T. Blaskovits and M. Leclerc, *J. Am. Chem. Soc.*, 2016, **138**, 10056–10071.
7 Y. Geng, Y. Chen, M. Du, H. Wu, Z. Ma, B. Xiao, H. Wang, A. Tang, X. Sun, Y. Zhong and E. Zhou, *Adv. Energy Mater.*, 2024, **14**, 2303976.
8 Y. Li, Y. Zhang, B. Wu, S. Pang, X. Yuan, C. Duan, F. Huang and Y. Cao, *Sol. RRL*, 2022, **6**, 2200073.
9 Y. Liu, K. Xian, R. Gui, K. Zhou, J. Liu, M. Gao, W. Zhao, X. Jiao, Y. Deng, H. Yin, Y. Geng and L. Ye, *Macromolecules*, 2022, **55**, 133–145.
10 Y. Liu, K. Xian, Z. Peng, M. Gao, Y. Shi, Y. Deng, Y. Geng and L. Ye, *J. Mater. Chem. A*, 2021, **9**, 19874–19885.
11 C. Yang, S. Zhang, J. Ren, M. Gao, P. Bi, L. Ye and J. Hou, *Energy Environ. Sci.*, 2020, **13**, 2864–2869.
12 J. Wu, Y. Xu, Z. Yang, Y. Chen, X. Sui, L. Yang, P. Ye, T. Zhu, X. Wu, X. Liu, H. Cao, A. Peng and H. Huang, *Adv. Energy Mater.*, 2018, **9**, 1803012.
13 K. Xian, Y. Liu, J. Liu, J. Yu, Y. Xing, Z. Peng, K. Zhou, M. Gao, W. Zhao, G. Lu, J. Zhang, J. Hou, Y. Geng and L. Ye, *J. Mater. Chem. A*, 2022, **10**, 3418–3429.
14 E. H. Jung, N. J. Jeon, E. Y. Park, C. S. Moon, T. J. Shin, T.-Y. Yang, J. H. Noh and J. Seo, *Nature*, 2019, **567**, 511–515.
15 X. Huang, X. Wang, Y. Zou, M. An and Y. Wang, *Small*, 2024, **20**, 2400874.
16 J. Wang, J. Liu, K. Zhou, K. Xian, Q. Qi, W. Zhao, Y. Chen and L. Ye, *Sol. RRL*, 2022, **6**, 2200779.
17 Y. Xiao, H. Wang, F. Awai, N. Shibayama, T. Kubo and H. Segawa, *ACS Appl. Mater. Interfaces*, 2022, **14**, 6994–7003.
18 M. Liu, O. Voznyy, R. Sabatini, F. P. Garcia de Arquer, R. Munir, A. H. Balawi, X. Lan, F. Fan, G. Walters, A. R. Kirmani, S. Hoogland, F. Laquai, A. Amassian and E. H. Sargent, *Nat. Mater.*, 2017, **16**, 258–263.
19 J. Liu, Y. Liu, J. Wang, H. Li, K. Zhou, R. Gui, K. Xian, Q. Qi, X. Yang, Y. Chen, W. Zhao, H. Yin, K. Zhao, Z. Zhou and L. Ye, *Adv. Energy Mater.*, 2022, **12**, 2201975.
20 J. Xu, O. Voznyy, M. Liu, A. R. Kirmani, G. Walters, R. Munir, M. Abdelsamie, A. H. Proppe, A. Sarkar, F. P. Garcia de Arquer, M. Wei, B. Sun, M. Liu, O. Ouellette, R. Quintero-Bermudez, J. Li, J. Fan, L. Quan, P. Todorovic, H. Tan, S. Hoogland, S. O. Kelley, M. Stefik, A. Amassian and E. H. Sargent, *Nat. Nanotechnol.*, 2018, **13**, 456–462.
21 D. Han, X. Yang, J. Liu and L. Ye, *ACS Appl. Polym. Mater.*, 2024, **6**, 14037–14046.
22 J. Salbeck, N. Yu, J. Bauer, F. Weissörtel and H. Bestgen, *Synth. Met.*, 1997, **91**, 209–215.
23 J. H. Heo, S. H. Im, J. H. Noh, T. N. Mandal, C.-S. Lim, J. A. Chang, Y. H. Lee, H.-j. Kim, A. Sarkar, M. K. Nazeeruddin, M. Grätzel and S. I. Seok, *Nat. Photonics*, 2013, **7**, 486–491.
24 S. Jia, C. Gu, X. Zhou, Y. Miao, Y. Tian, S. Wen, J. Ma and X. Bao, *Adv. Funct. Mater.*, 2025, DOI: 10.1002/adfm.202512747.
25 S. Y. Jeong, H. S. Kim and N. G. Park, *ACS Appl. Mater. Interfaces*, 2022, **14**, 34220–34227.
26 H. Liu, Y. Zhang, Z. Huang, Y. Wu, L. Wang, G. Liu, Y. Chen, K. Li, W. Zhang and H. Zhou, *Adv. Energy Mater.*, 2024, **14**, 2403737.
27 X. Wen, C. Gao, X. Ding, G. Shi, X. Yuan, B. Li, L. Yuan, J. Guo, C. Duan, Q. Shen, W. Ma and Z. Liu, *Adv. Mater.*, 2025, **37**, 2500562.
28 N. Yang, S. Zhang, Y. Cui, J. Wang, S. Cheng and J. Hou, *Nat. Rev. Mater.*, 2025, **10**, 404–424.
29 M. Liu, Y. Chen, C. S. Tan, R. Quintero-Bermudez, A. H. Proppe, R. Munir, H. Tan, O. Voznyy, B. Scheffel, G. Walters, A. P. T. Kam, B. Sun, M. J. Choi, S. Hoogland, A. Amassian, S. O. Kelley, F. P. Garcia de Arquer and E. H. Sargent, *Nature*, 2019, **570**, 96–101.
30 L. Ye, J. Wu, S. Catalan-Gomez, L. Yuan, R. Sun, R. Chen, Z. Liu, J. M. Ulloa, A. Hierro, P. Guo, Y. Zhou and H. Wang, *Nat. Commun.*, 2024, **15**, 7889.
31 Y. Ding, L. Zhang, P. Xie, Z. Zhang, G. Qu and Z. X. Xu, *Adv. Energy Mater.*, 2025, DOI: 10.1002/aenm.202504647.
32 Z. Xiong, Q. Zhang, K. Cai, H. Zhou, Q. Song, Z. Han, S. Kang, Y. Li, Q. Jiang, X. Zhang and J. You, *Science*, 2025, **390**, 638–642.
33 Y. Liu, K. Xian, X. Zhang, M. Gao, Y. Shi, K. Zhou, Y. Deng, J. Hou, Y. Geng and L. Ye, *Macromolecules*, 2022, **55**, 3078–3086.
34 Z. Peng, L. Ye and H. Ade, *Mater. Horiz.*, 2022, **9**, 577–606.
35 D. Bi, L. Yang, G. Boschloo, A. Hagfeldt and E. M. Johansson, *J. Phys. Chem. Lett.*, 2013, **4**, 1532–1536.
36 N. Y. Nia, F. Matteocci, L. Cina and A. Di Carlo, *ChemSusChem*, 2017, **10**, 3854–3860.
37 N. Yaghoobi Nia, M. Bonomo, M. Zendehdel, E. Lamanna, M. M. H. Desoky, B. Paci, F. Zurlo, A. Generosi, C. Barolo, G. Viscardi, P. Quagliotto and A. Di Carlo, *ACS Sustain. Chem. Eng.*, 2021, **9**, 5061–5073.
38 J. Wu, Y. Gao, Z. Zhou, Y. Du, J. Liu, J. Wang, Q. Wang, K. Zhou, K. Xian, Z. Lin, Y. Chen, W. Zhao, S. Li,

V. Kuvondikov, H. Yin, J. Yan, Y. Liu and L. Ye, *Adv. Funct. Mater.*, 2024, **34**, 2308584.
39 J. Sun, Y. Jin, Q. Liu and F. Qiu, *Chem.–Eng. J.*, 2023, **457**, 141300.
40 M.-H. Li, S. Wang, X. Ma, R. Long, J. Wu, M. Xiao, J. Fu, Z. Jiang, G. Chen, Y. Jiang and J.-S. Hu, *Joule*, 2023, **7**, 2595–2608.
41 M.-H. Li, X. Ma, J. Fu, S. Wang, J. Wu, R. Long and J.-S. Hu, *Energy Environ. Sci.*, 2024, **17**, 5513–5520.
42 M. J. Jeong, S. W. Jeon, S. Y. Kim and J. H. Noh, *Adv. Energy Mater.*, 2023, **13**, 2300698.
43 W. Ren, J. Ren, Y. Wu, S. Li, Q. Sun and Y. Hao, *Adv. Funct. Mater.*, 2024, **34**, 2311260.
44 L. Qi, G. Du, G. Zhu, Y. Wang, L. Yang and J. Zhang, *ACS Appl. Mater. Interfaces*, 2023, **15**, 41109–41120.
45 H. Choi, H. Lim, H. Kim, J. Lim, M. Park, C. S. Pathak and S. Song, *J. Mater. Chem. A*, 2023, **11**, 16363–16369.
46 J. Song, H. Xie, E. L. Lim, Y. Li, T. Kong, Y. Zhang, X. Zhou, C. Duan and D. Bi, *Sol. RRL*, 2022, **6**, 2100880.
47 W.-M. Gu, K.-J. Jiang, F. Li, G.-H. Yu, Y. Xu, X.-H. Fan, C.-Y. Gao, L.-M. Yang and Y. Song, *Chem.–Eng. J.*, 2022, **444**, 136644.
48 W. Li, H. Xu, G. Wang, W. Deng, Y. Long, X. Li, Y. Deng, H. Zhu, C. Wang, L. Xiao and Z. Zhong, *Chem.–Eng. J.*, 2025, **520**, 165687.
49 R. Roy, M. M. Byranvand, M. R. Zohdi, T. Magorian Friedlmeier, C. Das, W. Hempel, W. Zuo, M. Kedia, J. J. Rendon, S. Boehringer, B. Hailegnanw, M. Vorochta, S. Mehl, M. Rai, A. Kulkarni, S. Mathur and M. Saliba, *Energy Environ. Sci.*, 2025, **18**, 1920–1928.
50 F. Cheng, R. He, S. Nie, C. Zhang, J. Yin, J. Li, N. Zheng and B. Wu, *J. Am. Chem. Soc.*, 2021, **143**, 5855–5866.
51 J. Tong, C. Dong, M. Yao, Q. Wang, C. Shen, Y. Yue, L. Yan, Y. Gao, G. Yue, W. Zhang, M. I. Saidaminov and F. Tan, *ACS Nano*, 2025, **19**, 12960–12970.
52 M. H. Li, S. C. Liu, F. Z. Qiu, Z. Y. Zhang, D. J. Xue and J. S. Hu, *Adv. Energy Mater.*, 2020, **10**, 2000501.
53 W. Zhang, L. Wan, S. Fu, X. Li and J. Fang, *J. Mater. Chem. A*, 2020, **8**, 6546–6554.
54 Y. Li, X. Lu, Y. Mei, C. Dong, D. T. Gangadharan, K. Liu, Z. Wang, S. Qu, M. I. Saidaminov, W. Zhang and F. Tan, *Adv. Funct. Mater.*, 2023, **33**, 2301920.
55 H.-C. V. Tran, W. Jiang, M. Lyu and H. Chae, *J. Phys. Chem. C*, 2020, **124**, 14099–14104.
56 M. J. Jeong, K. M. Yeom, S. J. Kim, E. H. Jung and J. H. Noh, *Energy Environ. Sci.*, 2021, **14**, 2419–2428.
57 M. H. Li, J. Y. Shao, Y. Jiang, F. Z. Qiu, S. Wang, J. Zhang, G. Han, J. Tang, F. Wang, Z. Wei, Y. Yi, Y. W. Zhong and J. S. Hu, *Angew. Chem., Int. Ed.*, 2021, **60**, 16388–16393.
58 P. Lv, Y. Zhang, W. L. Tan, J. Pan, Y. Zhu, J. Chen, B. Duan, P. Hou, M. Hu, C. R. McNeill, J. Lu and Y.-B. Cheng, *J. Energy Chem.*, 2025, **108**, 477–484.
59 D. Xu, Z. Gong, Y. Jiang, Y. Feng, Z. Wang, X. Gao, X. Lu, G. Zhou, J.-M. Liu and J. Gao, *Nat. Commun.*, 2022, **13**, 7020.
60 F. Cao, F. Cheng, X. Huang, X. Dai, Z. Tang, S. Nie, J. Yin, J. Li, N. Zheng and B. Wu, *Adv. Funct. Mater.*, 2022, **32**, 2201423.
61 S. N. Habisreutinger, T. Leijtens, G. E. Eperon, S. D. Stranks, R. J. Nicholas and H. J. Snaith, *Nano Lett.*, 2014, **14**, 5561–5568.
62 J. Xiao, J. Shi, H. Liu, Y. Xu, S. Lv, Y. Luo, D. Li, Q. Meng and Y. Li, *Adv. Energy Mater.*, 2015, **5**, 1401943.
63 Y. Liu, B. He, J. Duan, Y. Zhao, Y. Ding, M. Tang, H. Chen and Q. Tang, *J. Mater. Chem. A*, 2019, **7**, 12635–12644.
64 J. Peng, D. Walter, Y. Ren, M. Tebyetekerwa, Y. Wu, T. Duong, Q. Lin, J. Li, T. Lu, M. A. Mahmud, O. L. C. Lem, S. Zhao, W. Liu, Y. Liu, H. Shen, L. Li, F. Kremer, H. T. Nguyen, D.-Y. Choi, K. J. Weber, K. R. Catchpole and T. P. White, *Science*, 2021, **371**, 390–395.
65 H. Kim, D. Y. Lee, J. Lim, J. Kim, J. Park, J. Seidel, J. S. Yun and S. I. Seok, *Adv. Energy Mater.*, 2023, **13**, 2301046.
66 Q. Qi, J. Wang, M. Gao, H. Ke, W. Zhao, K. Zhang, S. Li, C. He, V. Kuvondikov and L. Ye, *Small*, 2024, **20**, 2307993.
67 Z. Yao, Q. Xia, J. Li, X. Meng, Z. Huang, M. B. K. Niazi, S. Zhang, X. Hu and Y. Chen, *Aggregate*, 2025, **6**, e70017.
68 N. Li, A. Feng, X. Guo, J. Wu, S. Xie, Q. Lin, X. Jiang, Y. Liu, Z. Chen and X. Tao, *Adv. Energy Mater.*, 2022, **12**, 2103241.
69 J. Tong, C. Dong, V. M. Arnal, M. Yao, Q. Wang, Y. Song, Y. Deng, Y. Gao, G. Yue, W. Zhang, M. I. Saidaminov and F. Tan, *Chem. Eng. J.*, 2024, **501**, 157577.
70 J. Zhang, G. Zhang, Y. Liao, Z. Pan, H. Rao and X. Zhong, *Chem. Eng. J.*, 2023, **453**, 139842.
71 A. M. Risqi, M. Hu, L. Chen, B. w. Park, J. Park, J. Kim, Z. Yang and S. I. Seok, *Adv. Energy Mater.*, 2024, **15**, 2403033.
72 J. Zuo, D. Han, H. Yao, V. Kuvondikov and L. Ye, *Energy Environ. Sci.*, 2025, **18**, 6344–6365.
73 Y. Bai, S. M. Li, Q. Y. Wang, Q. Chen, Z. Zhang, S. X. Meng, Y. Zang, H. Y. Fu, L. W. Xue, L. Ye and Z. G. Zhang, *Natl. Sci. Rev.*, 2025, **12**, nwaf019.
74 Y. Bae, S. A. Park, S. Kim, H. Lim, J. Kim, L. Ye and T. Park, *Adv. Energy Mater.*, 2025, **15**, 2405217.
75 K. Zhou, D. Han, K. Xian, S. Li, M. Gao, K. Zhang, B. Zhao, X. Li, Y. Chen, Y. Geng and L. Ye, *Energy Environ. Sci.*, 2024, **17**, 5950–5961.
76 S. Li, M. Gao, K. Zhou, X. Li, K. Xian, W. Zhao, Y. Chen, C. He and L. Ye, *Adv. Mater.*, 2024, **36**, 2307278.
77 S. Li, J. Liu, V. Kuvondikov, J. Yan and L. Ye, *Matter*, 2025, **8**, 102062.
78 K. Xian, K. Zhou, M. Li, J. Liu, Y. Zhang, T. Zhang, Y. Cui, W. Zhao, C. Yang, J. Hou, Y. Geng and L. Ye, *Chin. J. Chem.*, 2023, **41**, 159–166.
79 K. Zhang, M. Gao, J. Wu, C. Sun, W. Zhao, D. Urazkulova, V. Kuvondikov, S. Nematov and L. Ye, *Mater. Horiz.*, 2025, **12**, 8832–8861.
80 Y. Zhang, P. Peng, Y. Xu, J. Wang, B. Xiao, V. Kuvondikov, S. Nematov, L. Ye and J. Liu, *Chin. J. Chem.*, 2026, **44**, 95–103.
81 K. Xian, R. Ma, K. Zhou, J. Liu, M. Gao, W. Zhao, M. Li, Y. Geng and L. Ye, *Aggregate*, 2024, **5**, e466.
82 J. Qiao, Q. Wang, J. Wang, J. Liu, W. Zhang, X. Liao, L. Ye, H. Yin and X. Hao, *Aggregate*, 2025, **6**, e722.
83 Y. Yang, K. Zhang, V. Kuvondikov, Y. Deng and L. Ye, *Chin. J. Chem.*, 2026, DOI: 10.1002/cjoc.70410.